International Journal of Thermophysics, Vol. 7, No. 1, 1986

Precise Measurements of Critical Parameters of Sulfur Hexafluoride by Laser Interferometry[1]

K. Morofuji,[2] K. Fujii,[2,3] M. Uematsu,[2] and K. Watanabe[2]

A laser interferometry has been applied, in the present study, for determination of the critical temperature and critical exponents of sulfur hexafluoride (SF_6). By means of laser holographic technique by real-time method, a series of Fraunhofer diffraction patterns due to the density fluctuation of the sample fluid in the very vicinity of the critical point has been successively photographed and analyzed. A dual-thermostat system which was designed and constructed for the present purpose has made the sample temperature constant within 15 μK for several days. We have obtained 107 data for $(\rho_L - \rho_V)/\rho_c$ along the vapor–liquid coexistence curve in the reduced temperature range $10^{-6} \leqq |\Delta T^*| \leqq 7 \times 10^{-5}$ and additional 34 data for the isothermal compressibility in the single phase region. By analyzing these measurements with the aid of the simple power law, the critical temperature and the critical exponents of SF_6 have been determined as $T_c = 318.708 \pm 0.001$ K, $\beta = 0.350 \pm 0.004$, and $\gamma = 1.24 \pm 0.02$, respectively.

KEY WORDS: critical exponent; critical parameter; gravity effect; laser interferometry; sulfur hexafluoride.

1. INTRODUCTION

Pure fluid in the vicinity of the vapor–liquid critical point exhibits significant fluctuation in the order parameter, i.e., density, in accord with the critical-point phase transition. The objective of the present study is to measure the density fluctuation of the fluid in the critical region by means of the laser holographic real-time method. A dual-thermostat system with a precise temperature regulation system has been designed and it becomes feasible to regulate the sample fluid temperature within 15 μK for a suf-

[1] Paper presented at the Ninth Symposium on Thermophysical Properties, June 24–27, 1985, Boulder, Colorado, U.S.A.

[2] Department of Mechanical Engineering, Keio University, Yokohama 223, Japan.

[3] Present address: National Research Laboratory of Metrology, Ibaraki 305, Japan.

0195-928X/86/0100-0017$05.00/0

ficiently long duration throughout the measurements. The Fraunhofer diffraction patterns of sulfur hexafluoride (SF_6) have been photographed successively along the vapor–liquid coexistence curve to the very vicinity of the critical point in the range of reduced temperatures $10^{-6} \leqq |(T - T_c)/T_c| \leqq 7 \times 10^{-5}$. Based upon a simple power-law analysis of the experimental results, the critical temperature and the critical exponents of SF_6 have been determined and are discussed in this paper.

2. PRINCIPLE OF MEASUREMENTS

When the thermodynamic state condition of a pure fluid approaches the vapor–liquid critical point, the isothermal compressibility of the fluid diverges, leading to a large density variation near the critical density due to the effect of the gravitational field. It has been well understood that the Fraunhofer diffraction pattern is formed when a thin slab of the fluid is illuminated by a plane-wave laser beam. Some of the earlier applications of this principle for the study of large density variation of fluids in the critical region have been reported [1–4].

The isothermal compressibility, κ_T, is defined as

$$\kappa_T = \rho^{-1}(\partial\rho/\partial P)_T \tag{1}$$

and the symmetrized isothermal compressibility, χ_T, is defined by the following expression,

$$\chi_T = (\partial\rho/\partial\mu)_T = \rho^2\kappa_T \tag{2}$$

where ρ denotes density, P pressure, T temperature, and μ chemical potential. Based upon the fundamental optics as for the generalization of Snell's law to the light propagation in a stratified medium (thickness d), and assuming that the angle of deflection, θ, is small, it becomes clear that the nondimensionalized isothermal compressibility, χ_T^*, is proportional to θ by the following expression,

$$\chi_T^* = \chi_T P_c/\rho_c^2 = H_0\theta/(Cd) \tag{3}$$

where H_0 and C are

$$H_0 = P_c/(\rho_c g) \tag{4}$$

$$C = (n_c^2 - 1)(n_c^2 + 2)/(6n_c) \tag{5}$$

Here P_c stands for the critical pressure, ρ_c the critical density, g the gravitational acceleration, and n_c the refractive index of the fluid at the

critical point. It is also conventionally accepted to reduce the order parameter $\Delta\rho = \rho - \rho_c$ and the ordering field $\Delta\mu = \mu(\rho, T) - \mu(\rho_c, T)$ into dimensionless quantities by the following definitions:

$$\Delta\rho^* = (\rho - \rho_c)/\rho_c \tag{6}$$

$$\Delta T^* = (T - T_c)/T_c \tag{7}$$

$$\Delta\mu^* = \Delta\mu\rho_c/P_c \tag{8}$$

Suppose that we could have the Fraunhofer diffraction pattern on the focal plane due to the laser interferometry and let I be the fringe number of the diffraction pattern. The reduced chemical potential, $\Delta\mu^*$, is related to $\Delta\rho^*$ and χ_T^* as

$$\Delta\rho^* - \chi_T^* \Delta\mu^* = \lambda(2I - 1)/(4Cd) \tag{9}$$

where λ denotes the wave length of the laser beam.

With respect to the pure fluid under the vapor–liquid coexistence at temperatures below the critical temperature, the fringes of the pattern corresponding to the maximum deflection angle disappear one after another as the fluid temperature decreases, since the density distribution is discontinuous at the vapor–liquid interface. Let I_{min} be such a minimum number of fringes; we can have the following relation,

$$(\rho_L - \rho_V)/\rho_c = \lambda(2I_{min} - 1)/(2Cd) \tag{10}$$

where ρ_L is the saturated liquid density and ρ_V the saturated vapor density.

3. EXPERIMENTAL APPARATUS AND PROCEDURE

A cross-sectional view of the sample cell used in the present study and its components are illustrated in Fig. 1. The sample fluid is confined within a small space of about 0.34 cm^3 in its inner volume. The space is constructed with two parallel synthetic sapphire windows and a Kovar ring. The sapphire windows are 12 mm in thickness and 20 mm in diameter and their two side surfaces are optically flat within $\lambda/4$. The Kovar ring (20-mm o.d., 12-mm i.d.) is 3.09 mm thick and a stainless-steel capillary (1.6-mm o.d., 0.8-mm i.d.) is soldered on it for the evacuation of the sample space as well as sample filling. A high-pressure valve (HIP-15-11AF1) is connected to the other end of the capillary. The gold packings (30 μm in thickness) are used for the seal between the sapphire windows and the Kovar ring. All of the components are tightened together by means of two flanges with the aid of the through bolts. A well for inserting a 25-Ω capsule platinum resistance thermometer is also provided in one of the flanges.

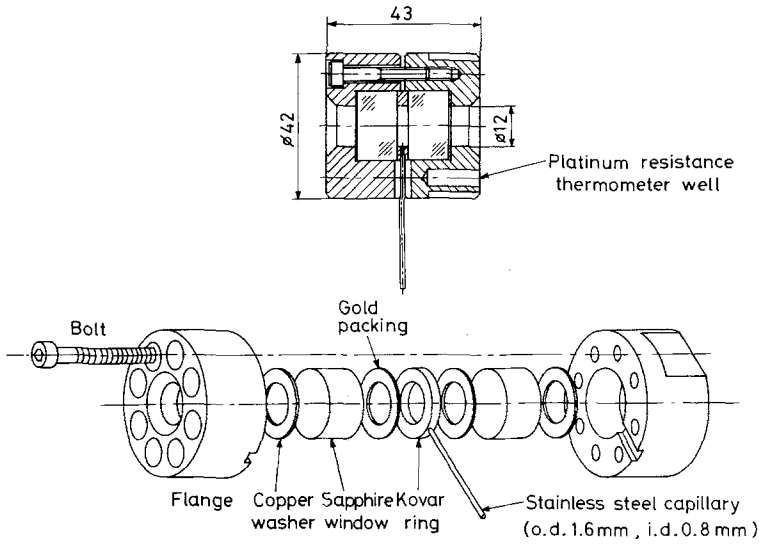

Fig. 1. Sample cell.

A dual-thermostat system is employed in the present study. The sample cell is installed in the middle of a thick-walled aluminum block on whose outer surface the silicone-rubber heaters are provided as shown in Fig. 2. The evacuated thermal insulation ($\sim$0.1 mPa) and associated copper tubings wound along the outer surface of the insulation are employed for the primary thermostat. The commercial heated-water circulator supplies the heated water, whose temperature is regulated at a temperature about 0.4 K higher than the prescribed sample temperature within a fluctuation of 0.03 K. As for the secondary temperature regulation, a thermistor installed into the aluminum block is used as a detector so as to control the supplying voltage to the silicone-rubber heaters. The side walls of the present dual thermostat are thermally insulated with the aid of foamed polyurethane plates. At the center of the insulated plates there exists a cylindrical space with four optical windows through which the laser beam traverses. The outermost space of the dual thermostat is also thermally insulated with glass wool. The horizontal level of the thermostat system is adjusted by the tripod screws.

A schematic diagram of the present temperature regulation systems is shown in Fig. 3. The thermistor (100 kΩ at 298 K with a temperature coefficient of 0.04 K^{-1}), R_T, serves as an arm of an AC Wheatstone bridge which is excited by 5-V voltage with 400-Hz frequency via an isolation transformer, T. A precision standard resistor (100 kΩ at 298 K, with a very

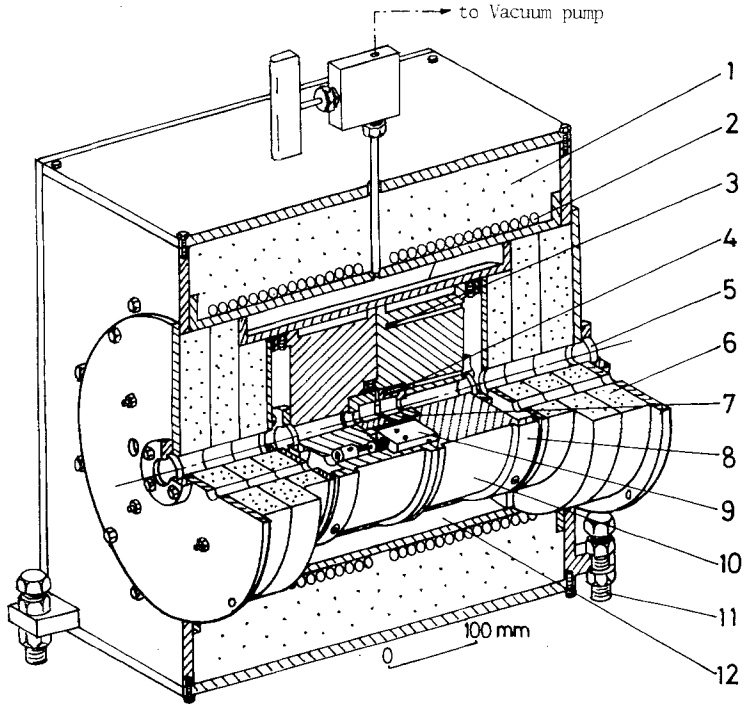

1:Insulator, 2:Copper tubings for circulating primary thermostated fluid,
3:Thermistor, 4:Platinum resistance thermometer, 5:Optical windows,
6:Insulator, 7:Sample cell, 8:Aluminum block, 9:Valve,
10:Silicon rubber heaters, 11:Tripod screws, 12:Evacuated thermal insulation

Fig. 2. Dual-thermostat system with the sample cell.

minute temperature coefficient of $0.6 \times 10^{-6}\ K^{-1}$), R_0, serves as a reference arm of the bridge, while the other two arms serve as a ratio transformer. The error signal from the bridge is amplified by a lock-in amplifier so as to generate the noise-eliminated DC voltage proportional to the temperature fluctuation. The error voltage is then input to a PID controller, whose output serves as the control signal of a DC power supplier in order to provide DC power of about 250 mW to the rubber heaters mentioned previously. The sample-fluid temperature can be chosen arbitrarily at 10-μK intervals by means of this temperature regulation system. The temperature of the sample fluid within the cell is detected by the capsule platinum resistance thermometer with an estimated uncertainty of 0.2 mK with the aid of a

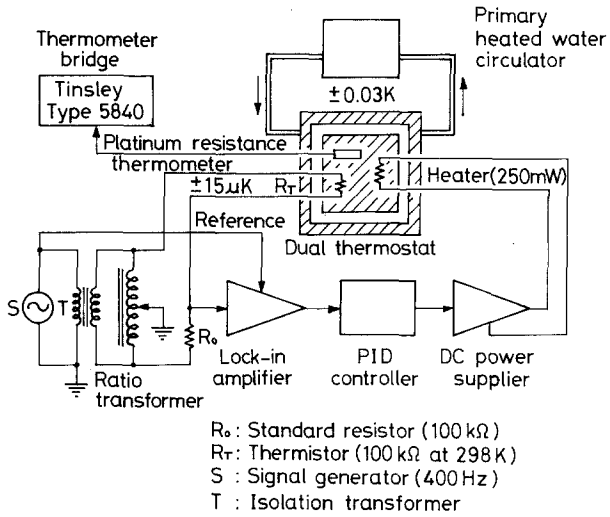

Fig. 3. Temperature regulation system.

thermometer bridge (Tinsley Type 5840). The thermometer itself has been calibrated on the IPTS-68 at the National Research Laboratory of Metrology, Ibaraki, with an estimated precision of 0.5 mK. The triple point of pure water was measured periodically by the thermometer used in the present study. These temperature regulating and measuring equipments, i.e., the PID controller, the standard precision resistor, and the Tinsley bridge, are placed in a temperature-controlled air bath at 295.0 ± 0.5 K.

A schematic diagram of the arrangement of the optical systems is shown in Fig. 4. The principle of the present measurements is the application of so-called laser holographic technique by the real-time

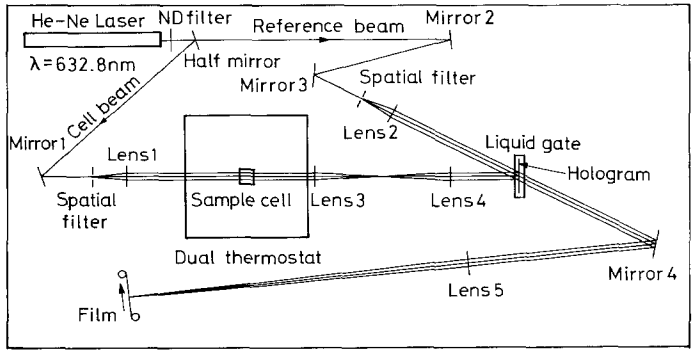

Fig. 4. Arrangement of the optical systems.

method so as to compensate possible optical distortions of the sapphire windows as well as those due to unavoidable unevenness of the mirrors, lenses, and so on. We have employed a 5-mW He–Ne laser ($\lambda = 632.8$ nm) as the light source and the emitted laser beam is, first, reduced in power to 0.3% by a neutral-density filter (ND filter) in order to prevent an unnecessary temperature increase in the fluid within the sample cell. Then the laser beam is split into the cell beam and the reference beam, where the former corresponds to the beam passing through the sample cell and the latter is the beam passing through the ambient air as shown in Fig. 4. Each split laser beam becomes the plane wave through the spatial filter associated with a lens and the matching of the total optical path length of each split beam between the half mirror and the liquid gate is carefully considered. A photographic plate immersed in a liquid gate is simultaneously illuminated by a focused image of the fluid after transmission through the sample cell and a coherent plane reference beam. The Fraunhofer diffraction patterns are then consecutively photographed on a film transported at a rate of about 1 cm · h^{-1}. All of the optical setup including the dual thermostat is surrounded by a blackout curtain and mounted on a surface plate (1×2 m) supported by the pneumatic vibration damper.

Prior to the measurements, the sample fluid of SF_6, 99.999 wt% in purity, is filled into the sample cell and its mass adjusted to the critical density. When the sample is heated up to the temperature around 1.3 K above the critical, where SF_6 is kept at the single phase state with a homogeneous density distribution, the initial hologram is recorded. After development, when the resulting hologram is illuminated by the cell beam alone, the cell beam diffracts toward mirror No. 4 (see Fig. 4). Then after decreasing the sample-fluid temperature to a temperature close enough to the critical, we have kept the sample temperature constant for over 14 h until the Fraunhofer diffraction patterns, without the constant phase distortion, are photographed consecutively on the film. The sample temperature was kept constant within a fluctuation of 15 μK for more than several hours. The temperature was varied stepwise by 0.7 mK.

4. EXPERIMENTAL RESULTS AND DISCUSSION

The temperature regulation system developed in the present study has kept the sample-fluid temperature constant at around the critical temperature of SF_6 within 15 μK for several days as far as it has been monitored by thermistor. We have assumed that the measured temperature of SF_6 is represented by the readings of the capsule platinum resistance thermometer, whereas the uniformity of the temperature regulation is monitored by the thermistor. In this connection the possible drift of the

thermistor readings discussed by Wilcox and Balzarini [1] was completely negligible and no effect on the diffraction patterns was observed throughout the present experiments. Drift of the reading of the capsule platinum resistance thermometer has been also calibrated by measuring resistance at the triple point of water. The observed difference before and after the present measurements for about 9 months was 0.1 mΩ, equivalent to 1 mK.

For the purpose of determining the vapor–liquid coexistence curve of SF_6 in the vicinity of the critical point, we have observed the diffraction patterns at 107 temperatures by seven different experimental runs in the reduced temperature range $10^{-6} \leqq |\Delta T^*| \leqq 7 \times 10^{-5}$. Based on these observations, we determined $(\rho_L - \rho_V)/\rho_c$ at respective temperatures. All of the observed data are plotted in the T vs $[(\rho_L - \rho_V)/\rho_c]^{1/\beta}$ diagram in Fig. 5, where a point of intersection of these data with the ordinate corresponds to the critical temperature, T_c. The aim of experimental runs 1 to 3 was to examine the effect of the meniscus level on the determination of the coexistence curve; the meniscus was kept at the central level in the case of

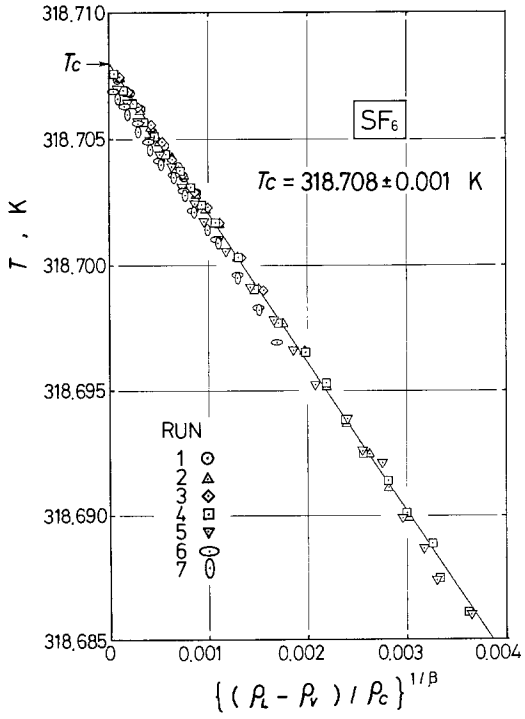

Fig. 5. T vs $[(\rho_L - \rho_V)/\rho_c]^{1/\beta}$ diagram.

run 2, whereas it was kept relatively at the upper and lower level in runs 1 and 3, respectively. It is noteworthy, however, that the intersecting points of them agree with each other within 0.1 mK. Experimental run 4 was conducted with newly refilled sample and results consistent with those of the preceding runs within 0.1 mK were found. About a month later, experimental run 5 was carried out with refilling of the sample and the results were lower in temperature by about 0.5 mK than those obtained in experimental runs through 1 to 4. Furthermore, about 3.5 months later, experimental runs 6 and 7 were carried out and the results also were lower in temperature by about 1 mK than those obtained in experimental runs through 1 to 4. In consideration of the drift of readings of the capsule platinum resistance thermometer, the corrected results of runs 5 to 7 were higher in temperature by about 0.5 or 1 mK. Note, however, that the uncorrected original results of runs through 5 to 7 are plotted in Fig. 5 for comparison of the results subject to the thermometer drifts. The following analysis of the critical temperature as well as the critical exponent β was conducted based on 61 data obtained by runs 1 to 4.

It is our current understanding that the simple power law is applicable to the generalized correlation of the coexistence curve of fluid in the form,

$$(\rho_L - \rho_V)/\rho_c = B\,|\Delta T^*|^{\beta} \tag{11}$$

where β and B are the critical exponent and amplitude of the coexistence curve, respectively. A logarithmic plot of the present results of runs 1 to 4 is shown in Fig. 6. A least-squares fitting applied to the present analysis gives $T_c = 318.708 \pm 0.001$ K and $\beta = 0.350 \pm 0.004$, taking into account the minimum chi-square (χ^2) distribution of the fitting. The error bars shown in Fig. 6 with respect to the value of $(\rho_L - \rho_V)/\rho_c$ reflect the estimated uncertainties, due mainly to the difficulties in identifying the number of fringes of the diffraction pattern, whereas those with respect to ΔT^* correspond to the experimental uncertainties of the temperature measurements, i.e., 0.2 mK, as discussed in the preceding section. The estimation of the possible uncertainties in the β value is rather difficult but we have adopted the standard deviation of β. The amplitude B due to the best fitting to Eq. (11) is 4.03 ± 0.20.

The critical parameters as well as the critical exponent β of SF_6 have been reported by various authors up to the present. Among the available T_c values, 318.70 K by Hocken and Moldover [5] and 318.718 K by Thijsse [6] have been obtained experimentally, whereas Ley-Koo and Green [7] reported 318.703 K due to their analysis of the experimental data on the static dielectric constant of SF_6 by Weiner et al. [8] The present result of $T_c = 318.708 \pm 0.001$ K is between these recent con-

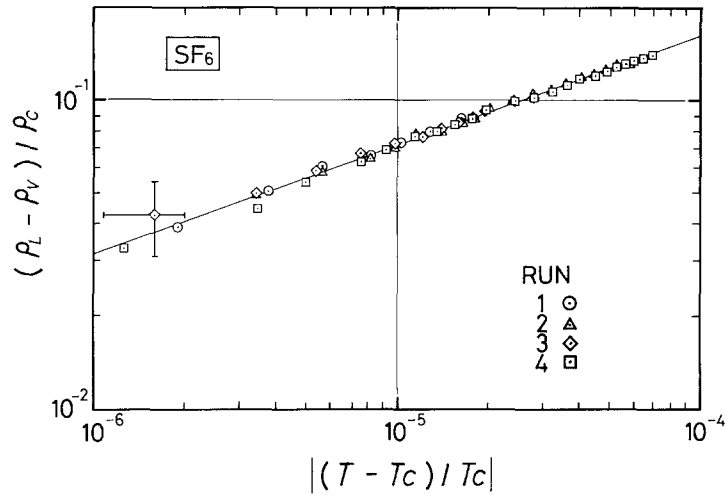

Fig. 6. Log–log plot of reduced density difference as a function of reduced temperature.

tributions but none of them overlap within their claimed uncertainties, although Hocken and Moldover [5] did not describe their claimed uncertainties. Most of the T_c values obtained by direct observation of the meniscus disappearance in earlier investigations [9–12] are several-tenths millikelvin higher than the present T_c. With respect to the discussion of the critical exponent β, Ley-Koo and Green [7] have pointed out that the simple power law would be applicable to the data available for the temperatures $|\Delta T^*| \leqq 7 \times 10^{-4}$. The temperature range of the present measurements, however, is up to about 7×10^{-5} in $|\Delta T^*|$, which is about one order of magnitude closer to the critical point than their proposed range. We have examined our data with the aid of two-term expansion and we found that there existed no significant contribution by adding the second term in our analysis. The present result for the amplitude B, on the other hand, coincides with the value of $B/2 = 1.74134 \pm 0.604$ reported by Ley-Koo and Green [7] within their claimed uncertainty but is slightly larger than that of Balzarini and Ohrn [13].

As for the isothermal compressibility in the single phase region, we have conducted three experimental runs (S1–S3) in the temperature range $10^{-5} \leqq |\Delta T^*| \leqq 7 \times 10^{-5}$ and have obtained 34 data along the critical isochore. The deflection angle, θ, of the laser beam in the sample cell increases on approaching the critical point and it becomes impossible to observe θ since the beam hits the peripheral edge of the window. This fact restricts the temperature range of measurements as above. We applied our

results to the simple power law in a functional form similar to that of Eq. (11),

$$\chi_T^* = \Gamma |\Delta T^*|^{-\gamma} \tag{12}$$

where γ and Γ are the critical exponent and amplitude of the isothermal compressibility, respectively. Using Eq. (12) the logarithmic plot of the present results after the corrections required for temperature is shown in Fig. 7, in which the straight line corresponds to the best fit. A least-squares fitting applied to the present analysis gives $\gamma = 1.24 \pm 0.02$ and $\Gamma = 0.040 \pm 0.012$, taking into account the minimum χ^2 distribution of the fitting. The associated uncertainties of γ and Γ have been evaluated from the possible errors in identifying the deflection angle of the fringe of the diffracted pattern, i.e., 1 mrad, and the resulting uncertainties in χ_T^* are shown as error bars in Fig. 7.

With respect to the critical exponent, γ, Hocken and Moldover [5] and Balzarini [14] have obtained experimentally $\gamma = 1.28$ and 1.18, respectively. The present result, $\gamma = 1.24 \pm 0.02$, is between those contributions.

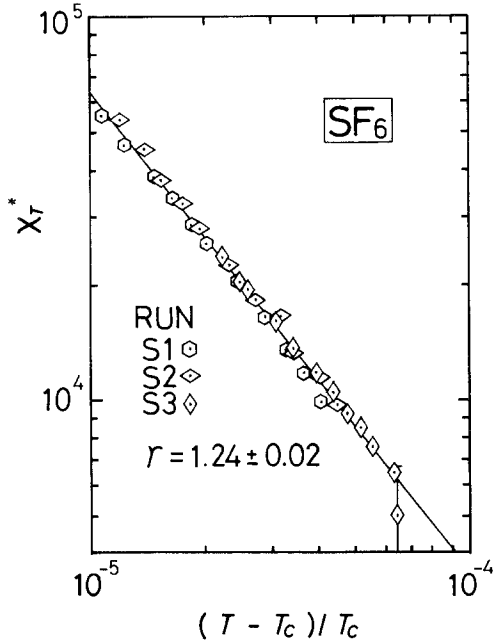

Fig. 7. Compressibility as a function of reduced temperature.

5. CONCLUSION

The precise determination of the critical temperature and related critical exponents for sulfur hexafluoride has been discussed in the present paper. The experimental results presented would contribute to further improvements in the development of theories to predict the anomalous thermodynamic behaviors of pure fluids in the vicinity of the critical point.

ACKNOWLEDGMENTS

The authors are grateful to Dr. R. Masui, National Research Laboratory of Metrology, Ibaraki, Japan, and also to Dr. T. Kashiwagi, Tokyo Institute of Technology, Tokyo, for their valuable advice in designing the present experimental setup. Dr. H. Sakurai, NRLM, Ibaraki, kindly calibrated the platinum resistance thermometer. Elaborate cooperation was given by T. Kanamori, former undergraduate student at Keio University. We were given the sample SF_6, of research-grade purity, by Asahi Glass Co., Ltd., Tokyo.

REFERENCES

1. L. R. Wilcox and D. Balzarini, *J. Chem. Phys.* **48**(2):753 (1968).
2. W. T. Estler, R. Hocken, T. Charlton, and L. R. Wilcox, *Phys. Rev. A* **12**(5):2118 (1975).
3. M. R. Moldover, J. V. Sengers, R. W. Gammon, and R. J. Hocken, *Rev. Mod. Phys.* **51**(1):79 (1979).
4. K. Fujii, M. Uematsu, and K. Watanabe, *Proc. 4th Japan Symp. Thermophys. Prop.* 171 (1983).
5. R. Hocken and M. R. Moldover, *Phys. Rev. Lett.* **37**(1):29 (1976).
6. B. J. Thijsse, *J. Chem. Phys.* **74**(8):4678 (1981).
7. M. Ley-Koo and M. S. Green, *Phys. Rev. Lett.* **29**(13):840 (1972).
8. Cited in Ref. 6.
9. H. P. Clegg, J. S. Rowlinson, and J. R. Sutton, *Trans. Faraday Soc.* **51**:1327 (1955).
10. R. H. Wentorf, Jr., *J. Chem. Phys.* **24**:607 (1956).
11. K. Kijima, M.S. thesis (Keio University, Yokohama, 1974).
12. D. Yu. Ivanov, L. A. Makarevich, and O. N. Sokolova, *JETP Lett.* **20**:121 (1974).
13. D. Balzarini and K. Ohrn, *Phys. Rev. Lett.* **29**(13):840 (1972).
14. D. A. Balzarini, *Can. J. Phys.* **50**:2174 (1972).